Alfred Stadler

Applications of the Covariant Spectator Theory

Received: date / Accepted: date

Abstract In this talk I provide a short overview of applications of the so-called Covariant Spectator Theory to two- and three-nucleon systems. It is a quasi-potential formalism based on relativistic quantum field theory, and can be derived from a reorganization of the complete Bethe-Salpeter series. In this framework, we constructed two one-boson-exchange models, called WJC-1 and WJC-2, for the neutron-proton interaction that fit the 2007 world data base, containing several thousands of neutron-proton scattering data below 350 MeV, with a $\chi^2/N_{\rm data}$ close to 1. The close fit to the observables implies that the phase shifts derived from these models can be interpreted as new phase-shift analyses, which can be used also in nonrelativistic frameworks. Both models have a considerably smaller number of adjustable parameters than are present in realistic nonrelativistic potentials, which shows that the inclusion of relativity actually helps to achieve a realistic description of the interaction between nucleons. This became also evident in calculations of the three-nucleon bound state, where the correct binding energy is obtained without additional irreducible three-body forces which are needed in nonrelativistic calculations. In addition, calculations of the electromagnetic form factors of helium-3 and of the triton in complete impulse approximation also give very reasonable results, demonstrating the Covariant Spectator Theory's ability to describe the structure of the three-nucleon bound states realistically.

Keywords Relativistic few-body systems · Nuclear interaction

1 Covariant Spectator Theory of Two- and Three-Nucleon Systems

The purpose of this talk is to give a brief overview of recent results we obtained in relativistic calculations of two-nucleon ($2N$) and three-nucleon ($3N$) systems in the framework of the covariant spectator theory (CST). As will be demonstrated, we found simple one-boson-exchange (OBE) models of the nucleon-nucleon (NN) interaction that provide a more efficient description of the NN observables than nonrelativistic models. This efficiency applies also to the $3N$ bound state, which can be well described without $3N$ forces. The obtained simplification depends crucially on relativity.

One way of introducing the two-body CST is to start from the manifestly covariant Bethe-Salpeter (BS) equation for the scattering amplitude M of two particles with masses m_1 and m_2, which can be written in the general form $M = V_{\rm BS} + V_{\rm BS} G_{\rm BS} M$, where $V_{\rm BS}$ is a complete kernel consisting of an infinite number of two-body-irreducible boson-exchange diagrams. The propagator $G_{\rm BS}$ is the product of the propagators of the two particles. This equation can then be recast into another equivalent form, $M = V_{\rm CST} + V_{\rm CST} G_{\rm CST} M$, in which a different propagator $G_{\rm CST}$ and an accordingly modified kernel $V_{\rm CST}$ is used. For the case of spin-1/2 particles,

Presented at LIGHTCONE 2011, 23 - 27 May, 2011, Dallas.

Stadler, A.
Departamento de Física da Universidade de Évora, 7000-671 Évora, Portugal
and Centro de Física Nuclear da Universidade de Lisboa, 1649-003 Lisboa, Portugal
E-mail: stadler@uevora.pt

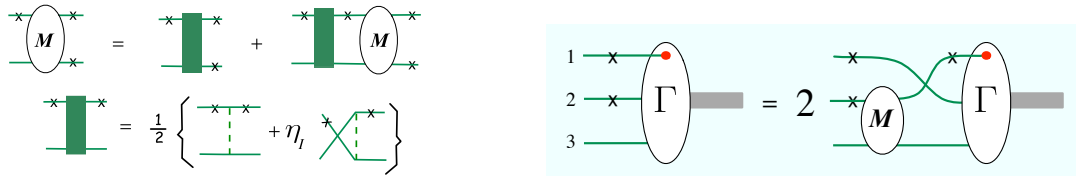

Fig. 1 On the left, a diagrammatic representation of the Covariant Spectator equation (2) with particle 1 on-shell (the on-shell particle is indicated with a $\times$). The second line shows the definition of the antisymmetrized kernel $\overline{V}_{12}$, with $\eta_I = (-)^I$, where I is the NN isospin. On the right, a diagramatic representation of the Covariant Spectator equation for the 3N bound state vertex function Γ with particles 1 and 2 on-shell (labeled with a $\times$). Here particle 1 is the spectator to the last two-body interaction between particles 2 and 3, described by the scattering amplitude M with particle 3 off-shell.

the replacement is

$$G_{\rm BS} = \frac{1}{m_1 - \not{p}_1}\frac{1}{m_2 - \not{p}_2} \quad \longrightarrow \quad G_{\rm CST} = 2\pi i \delta_+(m_1^2 - p_1^2)(m_1 + \not{p}_1)\frac{1}{m_2 - \not{p}_2}\,, \tag{1}$$

which places particle 1 in intermediate states on its mass shell [1–3]. This reduces the dimension of the integration over intermediate momenta from four to three, while maintaining the manifest covariance of the equation. The new kernel $V_{\rm CST}$ contains again an infinite number of diagrams, which are now two-body irreducible with respect to the propagator $G_{\rm CST}$. What originally motivated this choice of propagator was—apart from the simplification of the integrations—the existence of cancellations between ladder and crossed-ladder diagrams in scalar theories of ϕ^3-type, where two heavier particles with unequal masses exchange a third lighter one. Truncation of the kernel $V_{\rm CST}$ to OBE level is therefore expected to converge faster than the corresponding "ladder approximation" in the BS equation with $V_{\rm BS}$.

Also, unlike the BS equation in ladder approximation, the CST two-body equation has the correct one-body limit: when one particle becomes infinitely massive, the two-body equation reduces to a relativistic one-body equation for the light particle moving in an effective potential created by the massive particle.

For systems with more than two particles, the CST procedure places all particles but one on mass shell, which leads to a consistent description. For instance, the CST three-body equation satisfies the property of cluster-separability, without which a two-body CST amplitude could not be used consistently in the kernel of a three-body equation. For a brief recent review of the CST see Ref. [4].

In our applications to NN scattering, the specific form of the CST equation for the scattering amplitude of two nucleons with mass m, with particle 1 on-shell in both the initial and final state, is [5]

$$M_{12}(p,p';P) = \overline{V}_{12}(p,p';P) - \int \frac{d^3k}{(2\pi)^3}\frac{m}{E_k}\overline{V}_{12}(p,k;P)G_2(k,P)M_{12}(k,p';P)\,, \tag{2}$$

where P is the conserved total four-momentum, and p, p', and k are relative four-momenta related to the momenta of particles 1 and 2 by $p_1 = \frac{1}{2}P + p$, $p_2 = \frac{1}{2}P - p$, and M_{12} is the matrix element of the Feynman scattering amplitude between positive energy Dirac spinors of particle 1. The covariant kernel $\overline{V}_{12}$ (which is also referred to as the "potential") is explicitly antisymmetrized, ensuring that the amplitudes M_{12} satisfy the generalized Pauli principle. The propagator for the off-shell particle 2 is

$$G_2(k,P) \equiv G_{\beta\beta'}(k_2) = \frac{(m + \not{k}_2)_{\beta\beta'}}{m^2 - k_2^2 - i\varepsilon}\,h^2(k_2)\,, \tag{3}$$

with $k_2 = P - k_1$, $k_1^2 = m^2$. It is dressed by the off-shell nucleon form factor $h(k_2)$, which can be related to the self-energy of the off-shell nucleon, and which is normalized to unity when $k_2^2 = m^2$.

The propagator of an off-shell particle can be decomposed into positive and negative energy contributions, which separates the CST equations into positive- and negative-energy channels. Negative-energy states are related to the "Z-graphs" of time-ordered perturbation theory. In this sense, the solutions of (2) automatically include Z-graphs to all orders.

The CST equations for the 3N bound state were formulated in a way suitable for a practical solution in Ref. [6]. One obtains a homogeneous equation for the vertex function Γ of the 3N bound state, shown graphically in Fig. 1. All relativistic effects can be calculated *exactly* in CST, and the full Dirac structure of

the nucleons is also taken into account. The CST $3N$ equation was solved numerically for the first time in Ref. [7], for a family of older OBE potentials. Since then, much progress has been made in the development of more accurate CST NN interaction models, which will be described in the following section.

2 High-Precision np Kernels

The first covariant NN OBE kernels in CST, based on the exchange of either four or six mesons, were published in 1992 [5]. Since then, the applied numerical techniques and the structure of the kernels were gradually improved, and the np data base considerably enlarged. The two new models WJC-1 and WJC-2 [8] represent the most recent world np data with a precision that is on par with all commonly used "realistic" potentials.

The kernels are sums of OBE contributions. For bosons with incoming (outgoing) momenta k_i (p_i), the individual boson contributions are of the form

$$V_{12}^b(p,k;P) = \varepsilon_b \delta \frac{\Lambda_1^b(p_1,k_1)\otimes\Lambda_2^b(p_2,k_2)}{m_b^2+|q^2|} f(\Lambda_b,q)\,. \tag{4}$$

Here, $b=\{s,p,v,a\}$ denotes the boson type (scalar, pseudoscalar, vector, axial vector), $q=p_1-k_1=k_2-p_2=p-k$ the momentum transfer, m_b the boson mass, ε_b a phase factor, $\delta=1$ for isoscalar bosons and $\delta=\tau_1\cdot\tau_2=-1-2(-)^I$ for isovector bosons, and $f(\Lambda_b,q)$ a boson form factor depending on a form factor mass Λ_b. The axial vector bosons are treated as contact interactions, with a structure as in (4), but with the propagator replaced by a constant.

For example, the boson-nucleon vertex for scalar mesons is of the general form

$$\Lambda_i^s(p_i,k_i) = g_s - v_s\left[\frac{m-\not{p}_i}{2m}+\frac{m-\not{k}_i}{2m}\right], \tag{5}$$

where g_s and v_s are coupling constants. Note that terms proportional to v_s contribute only if the nucleon is off mass shell on at least one side of the vertex. These terms are therefore called "off-shell couplings." Similar couplings are included for vector and pseudoscalar meson exchanges. In the case of pseudoscalar exchange, the offshell coupling strength parametrizes a mixing between pseudoscalar and pseudovector coupling. For the detailed forms of all numerator functions $\Lambda_1^b\otimes\Lambda_2^b$ see Ref. [8].

The replacement of q^2 by $-|q^2|$ in the propagators and form factors is a covariant redefinition in the region $q^2>0$ that removes all singularities and can be justified by a detailed study of the structure of the exchange diagrams [8].

WJC-1 is our model with the best fit, whereas WJC-2 uses the smallest number of parameters without significantly deteriorating the quality of the fit. Table 1 shows that we achieved excellent fits for the most complete data base of np scattering, and with a considerably smaller number of adjustable parameters than other realistic potential models. In fact, in view of the $\chi^2/N_{\rm data}=1.06$ of model WJC-1, the corresponding phase shifts can be considered a new phase shift analysis which includes many more data than the "standard" Nijmegen 93 analysis [9] to which all realistic potential models were fitted. Note that our phase shifts, shown in Fig. 2, can be used outside the framework of CST, just like any other phase shift analysis.

Table 1 Comparison of precision np models and the 1993 Nijmegen phase shift analysis. The first column specifies the model, the second the number of adjustable parameters (in the case of the first four models for both np and pp data), and the third the year of the data base (data prior to this year are included). Columns four to six are the obtained $\chi^2/N_{\rm data}$ for various data bases (identified by their year), where the number of included data is given in parentheses. Our calculations are in bold face.

Model			$\chi^2/N_{\rm data}(N_{\rm data})$		
Reference	$N_{\rm pars}$	Year	1993	2000	2007
PWA93	39	1993	0.99(2514)	—	—
			1.09(3011)	**1.12**(3336)	**1.13**(3788)
Nijm I	41	1993	1.03(2514)	—	—
AV18	40	1995	1.06(2526)	—	—
CD-Bonn	43	2000	—	1.02(3058)	—
WJC-1	27	2007	**1.03**(3011)	**1.05**(3336)	**1.06**(3788)
WJC-2	15	2007	**1.09**(3011)	**1.11**(3336)	**1.12**(3788)

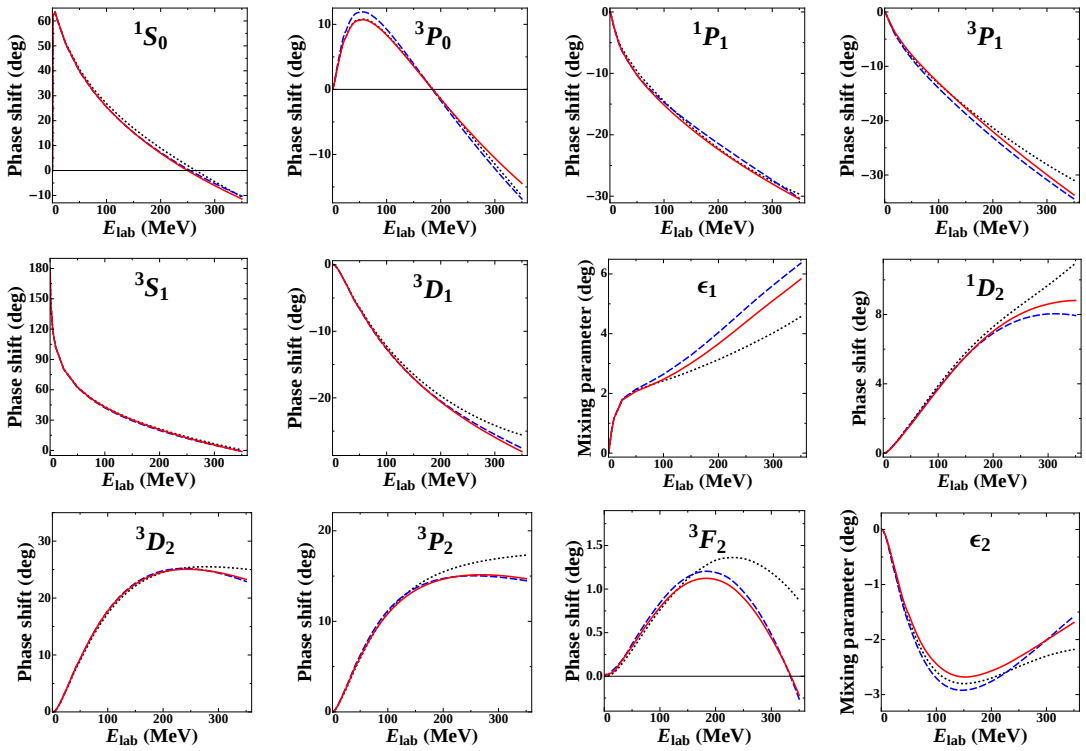

Fig. 2 Phase shifts of np scattering for partial waves with $J \leq 2$. The solid and dashed lines respresent the results of models WJC-1 and WJC-2, respectively. The dotted line shows the Nijmegen multienergy phase shift analysis of 1993[9].

The deuteron binding energy was used as a constraint during the fitting of the CST NN kernels, and therefore they reproduce the experimental binding energy of $E_d = 2.2246$ MeV automatically. The deuteron vertex functions can be related to the well-known nonrelativistic S- and D-state deuteron wave functions $u(p)$ and $w(p)$, respectively. In addition one obtains spin singlet and triplet P-waves, $v_s(p)$ and $v_t(p)$, which are of relativistic origin. Tables with the numerical values, and convenient parameterizations using analytic functions, both in momentum and coordinate space, are given in Ref. [10].

3 Three-Nucleon Binding Energies and Electromagnetic Form Factors

An interesting problem in few-nucleon physics is the inability of realistic NN potentials to explain the experimental triton binding energy $E_t = 8.48$ MeV. The potentials with the lowest $\chi^2/N_{\rm data}$ fits of the NN data produce binding energies between 7.6 and 8 MeV. A possible explanation is that $3N$ forces are not negligible. However, models for $3N$ forces introduce additional parameters which are usually adjusted to reproduce the triton binding energy, and therefore the calculations loose predictive power.

The CST calculations of Ref. [7] showed that the scalar off-shell coupling terms of Eq. (5) in a relativistic NN kernel not only improve the fit to the NN data, but the model with the best fit, called W16, also predicts the correct triton binding energy without $3N$ forces. These terms are not present in nonrelativistic theories because they require nucleons to go off mass shell. Surprisingly, both new high-precision models WJC-1 and WJC-2—with $E_t = 8.48$ MeV and $E_t = 8.50$ MeV, respectively—again predict the experimental binding energy very closely, even though their detailed structure and their parameters differ quite significantly from each other and from the old model W16. It appears unlikely that this is a mere coincidence. Figure 3 shows the changes in $\chi^2/N_{\rm data}$ and E_t when v_σ is held fixed at certain values while all other potential parameters are refitted, confirming the importance of this mechanism in our NN kernels.

Note that in a true relativistic OBE theory for the NN interaction, no additional irreducible $3N$ forces, which might spoil the nice agreement with the experimental value for E_t, can be derived from the basic vertices of the theory. However, it is important to remember that the concept of $3N$ forces is framework-dependent.

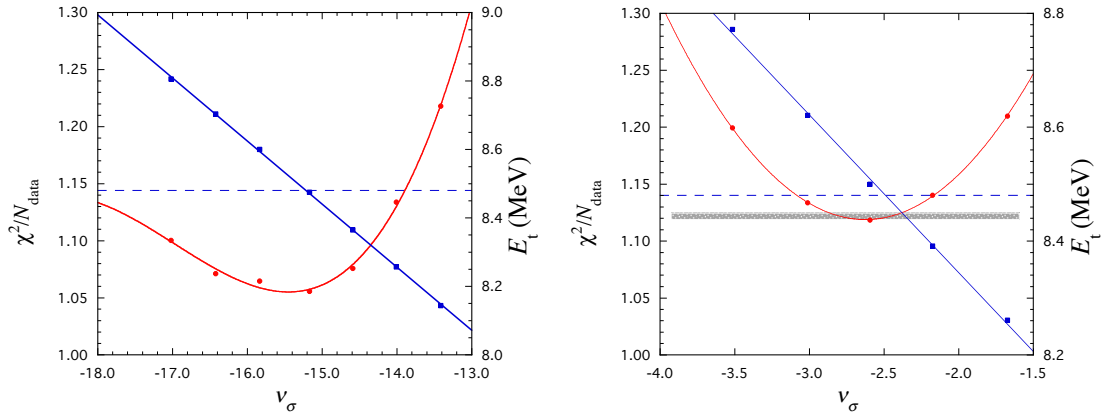

Fig. 3 Results for calculations of $\chi^2/N_{\rm data}$ (solid circles on curved line and left scale) to a 2007 *np* data base, and triton binding energy E_t (solid squares on straight line and right scale) for WJC-1 family (left panel) and for WJC-2 family of models (right panel). The points with the lowest $\chi^2/N_{\rm data}$ are models WJC-1 and WJC-2, respectively. The other models of the two families were obtained by fixing ν_σ at different values and refitting all other parameters. The curves are fits through the actually calculated points.

Figure 4 illustrates that vertices with off-shell terms together with off-shell propagators can transform into contact vertices and take the form of 3*N* forces. But in the framework of the CST they are *completely determined from the NN interaction* and automatically included through the OBE kernel. Our calculations provide true predictions of the triton binding energy and of the structure of the 3*N* bound state in the form of the 3*N* vertex function.

To test these vertex functions, we derived the conserved CST 3*N* current in [11], and calculated the electromagnetic form factors of the 3*N* bound states in "Complete Impulse Approximation" (CIA), first for an older family of ν_s-dependent *NN* potentials [12], and then also for the new high-precision models [13]. The term "impulse approximation" can be misleading because the CIA in CST includes contributions that in non-relativistic frameworks appear as interaction currents (pair terms related to Z-graphs). A good description of the data over a large range of Q cannot be expected in CIA, because interaction currents give important contributions to the 3*N* form factors. Therefore, we compare to calculations by the Pisa-Jlab collaboration, described in Ref. [14] and labeled "IARC" below. The IARC calculations use a nonrelativistic impulse approximation with a one-nucleon current and wave functions obtained from the Argonne AV18 *NN* and Urbana IX 3*N* potentials, and also include first-order relativistic corrections. The Coulomb interaction is not included in the IARC and CST calculations presented here.

Figure 5 shows the isoscalar and isovector charge and magnetic 3*N* form factors for models WJC-1 and WJC-2 in CIA-0 [13] (an approximation to CIA in which the 3*N* vertex function with two off-shell nucleons is replaced by a vertex function with only one nucleon off mass shell), W16 both in CIA and CIA-0, and IARC for the AV18/UIX interaction. Clearly, CIA-0 is an excellent approximation to CIA for W16. All models reproduce the correct 3*N* binding energy, and the form factors remain close to each other. Only WJC-1 shows some deviations already at relatively small Q. The reason for this behavior is instructive: WJC-1 is the only model with a mixed pseudoscalar-pseudovector πNN coupling. Its pseudoscalar part induces strong Z-graph-type currents, which are not present in the other cases.

The 3*N* electromagnetic form factors obtained with our relativistic kernels exhibit a very reasonable behavior. We can conclude that CST not only predicts the 3*N* binding energy correctly, but also yields a sound description of the structure of the 3*N* bound states.

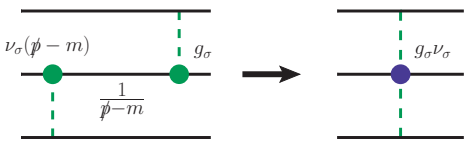

Fig. 4 Boson-nucleon vertices with off-shell coupling can generate effective 3*N* forces. In this example, an off-shell nucleon consecutively exchanges a scalar σ meson with two different nucleons. When a scalar off-shell vertex is multiplied with the nucleon propagator, the two separate boson-nucleon vertices shrink to a single contact vertex, and the whole diagram takes on the form of a 3*N* force.

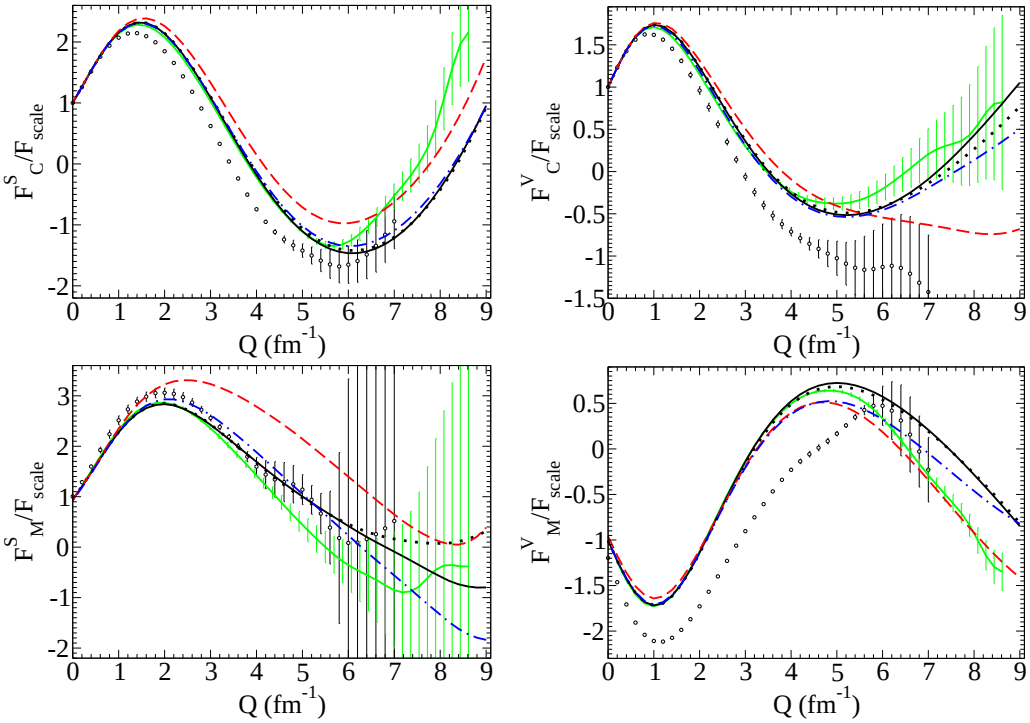

Fig. 5 Isoscalar (first row) and isovector (second row) charge form factors of the 3*N* bound states. In each case, the form factor is divided by a common scaling function $F_{\rm scale}(Q)$ [13]. The solid line is the result for *NN* model W16 in CIA, the dotted line is the approximation CIA-0 for the same model. The dashed line is model WJC-1, and the dash-dotted line is model WJC-2, both in CIA-0. For comparison, the solid line with theoretical error bars is the result of an IARC calculation by Marcucci based on the AV18/UIX potential. All calculations employ the on-shell single-nucleon current. The full circles represent the experimental data [15].

Acknowledgements This work is the result of a long-term collaboration with Franz Gross. The electromagnetic 3*N* form factors were calculated by S.A. Pinto. The author was supported by Fundação para a Ciência e a Tecnologia (FCT) under grant Nos. PTDC/FIS/113940/2009 and POCTI/ISFL/2/275.

References

1. Gross, F.: Three-Dimensional Covariant Integral Equations For Low-Energy Systems. Phys. Rev. **186**, 1448 (1969)
2. Gross, F.: Relativistic few-body problem. I. Two-body equations. Phys. Rev. C **26**, 2203 (1982)
3. Gross, F.: Relativistic few-body problem. II. Three-body equations and three-body forces. Phys. Rev. C **26**, 2226 (1982)
4. Stadler, A., Gross, F.: Covariant Spectator Theory: Foundations and Applications. Few-Body Syst. **49**, 91–110 (2011)
5. Gross, F., Van Orden, J.W., Holinde, K.: Relativistic one-boson-exchange model for the nucleon-nucleon interaction. Phys. Rev. C **45**, 2094 (1992)
6. Stadler, A., Gross, F., Frank, M.: Covariant equations for the three-body bound state. Phys. Rev. C **56**, 2396 (1997)
7. Stadler, A., Gross, F.: Relativistic calculation of the triton binding energy and its implications. Phys. Rev. Lett. **78**, 26 (1997)
8. Gross, F., Stadler, A.: Covariant spectator theory of *np* scattering: Phase shifts obtained from precision fits to data below 350 MeV. Phys. Rev. C **78**, 014005 (2008)
9. Stoks, V.G.J., Klomp, R.A.M., Rentmeester, M.C.M., de Swart, J.J.: Partial-wave analysis of all nucleon-nucleon scattering data below 350 MeV. Phys. Rev. C **48**, 792 (1993)
10. Gross, F., Stadler, A.: Covariant spectator theory of *np* scattering: Effective range expansions and relativistic deuteron wave functions. Phys. Rev. C **82**, 034004 (2010)
11. Gross, F., Stadler, A., Peña, M.T.: Electromagnetic interactions of three-body systems in the covariant spectator theory. Phys. Rev. C **69**, 034007 (2004)
12. Pinto, S.A., Stadler, A., Gross, F.: Covariant spectator theory for the electromagnetic three-nucleon form factors: Complete impulse approximation. Phys. Rev. C **79**, 054006 (2009)
13. Pinto, S.A., Stadler, A., Gross, F.: First results for electromagnetic three-nucleon form factors from high-precision two-nucleon interactions. Phys. Rev. C **81**, 014007 (2010)
14. Marcucci, L.E., Viviani, M., Schiavilla, R., Kievsky, A., Rosati, S.: Electromagnetic structure of A = 2 and 3 nuclei and the nuclear current operator. Phys. Rev. C **72**, 014001 (2005)
15. Sick, I.: Elastic Electron Scattering from Light Nuclei. Prog. Part. Nucl. Phys. **47**, 245 (2001)